IEICE Proceeding Series

# Performance Improvement of PID-DAC-Nonlinear-Compensator by Applying Online System Identification

Takanori Emaru, Hiroto Sasaki, Yohei Hoshino, Yukinori Kobayashi

Vol. 1 pp. 191-194
Publication Date: 2014/03/17
Online ISSN: 2188-5079

2012 International Symposium on Nonlinear Theory and its Applications
NOLTA2012, Palma, Majorca, Spain, October 22-26, 2012

# Performance Improvement of PID-DAC-Nonlinear-Compensator by Applying Online System Identification

Takanori Emaru†, Hiroto Sasaki‡, Yohei Hoshino† and Yukinori Kobayashi†

†Faculty of Engineering, Hokkaido University
N13W8, Sapporo-shi, Hokkaido, 060-8628 Japan
‡Graduate School of Engineering, Hokkaido University
Email: emaru@eng.hokudai.ac.jp

**Abstract**—In this paper we propose the performance improvement schemes for nonlinear controlled objects by applying online system identification. Generally, multi-body mechanical systems have high nonlinearity because of the influence of gravity, friction, interaction of joints, and other factors. Therefore, the accuracy of the Proportional-Integral-Derivative (PID) control is limited. In contrast, a digital acceleration control (DAC) method has robustness against modeling errors that are caused by such nonlinearity. A combined control system of PID and DAC (PID-DAC) has been proposed in our previous research and the validity of it has been confirmed. However, the PID-DAC control system cannot compensate for modeling errors of the inertia matrix or mass change of the controlled object. To solve this problem, we apply online system identification algorithm to the PID-DAC. The effectiveness of the proposed method is investigated through experiments on a two-link robot manipulator.

## 1. Introduction

The accuracy of the Proportional-Integral-Derivative (PID) control widely used by mechanical systems such as robot manipulators is limited by modeling errors caused by the influence of gravity, friction, and joint interaction. In comparison, Digital Acceleration Control [1] (DAC) is more robust against modeling errors and thus superior to PID.

DAC requires the information on positioning, velocity and acceleration to be precise. Velocity and acceleration can be obtained theoretically from positioning, without using sensors. This paper presents simulations and experimental results obtained using digital differentiator, ESDS [2, 3]. ESDS is one of the nonlinear filters that is based on sliding mode technique [4, 5]. By using ESDS, we can construct DAC system without increasing the number of sensors. A combined control system of PID and DAC (PID-DAC) which includes ESDS as a differentiator has been proposed in our previous research [6, 7]. However, the PID-DAC control system cannot compensate for modeling errors of the inertia matrix or mass change of the controlled object. To solve this problem, we apply an online system identification algorithm to the PID-DAC. We applied the proposed control system to a 2-link manipulator, and experimentally confirmed the validity of the proposed method. The results confirmed that the PID-DAC controller with system identification algorithm works as a nonlinear compensator properly.

## 2. Brief explanations of PID-DAC and ESDS

This section explains the combined control system of PID and DAC (PID-DAC) and nonlinear filter ESDS.

### 2.1. The PID-DAC control system construction

Controlling of the mechanical systems is affected by the modeling errors. Modeling errors cause reductions in accuracy. However, the digital acceleration control (DAC) [1] is robust to the modeling errors, and this paper presents a combined control system, the PID-DAC:

$$\begin{aligned}\boldsymbol{\tau}_{\mathrm{pidac}}(kT^+) &= \boldsymbol{\tau}_{\mathrm{pidac}}(kT^-)\\ &+\boldsymbol{M}[\boldsymbol{\theta}(kT^+)]\{\ddot{\boldsymbol{\theta}}_d(kT^+) - \ddot{\boldsymbol{\theta}}(kT^-)\}\\ &+\boldsymbol{K}_{\mathrm{p}}\boldsymbol{e}(t) + \boldsymbol{K}_{\mathrm{d}}\dot{\boldsymbol{e}}(t) + \boldsymbol{K}_{\mathrm{i}}\int_0^t \boldsymbol{e}(\alpha)d\alpha \end{aligned} \quad (1)$$

Equation (1) determines the input torque of the PID-DAC for controlling the angle of robot manipulator. Here, $\boldsymbol{\tau}_{\mathrm{pidac}}(kT^+)$ is an input torque at the time $t = kT^+$, $\boldsymbol{\tau}_{\mathrm{pidac}}(kT^-)$ is an input torque at the time $t = kT^-$ (the moment immediately before $t = kT^+$), $\boldsymbol{M}$ is inertia matrix, and $\boldsymbol{e}(t)$ is angular error. $\boldsymbol{K}_{\mathrm{p}}$, $\boldsymbol{K}_{\mathrm{i}}$, and $\boldsymbol{K}_{\mathrm{d}}$ are PID parameters.

### 2.2. Implementation of PID-DAC

DAC is an effective control method, however, additional sensors are needed to measure velocity and acceleration. Therefore, a system that Estimates the Smoothed and Differential values by a Sliding mode (ESDS) [2, 3] is employed to estimate the velocity and acceleration from rotational angle. In this subsection, the actual implementation of a differential estimator is described. The theorem for

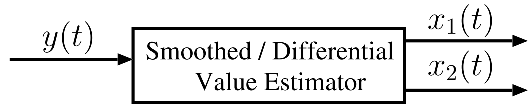


Figure 1: View of estimator

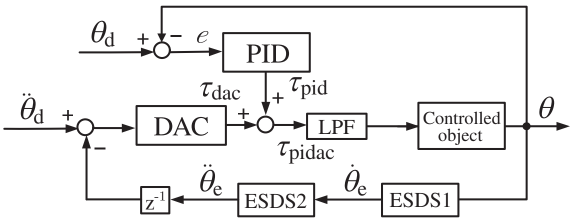

Figure 2: Block diagram of the PID-DAC

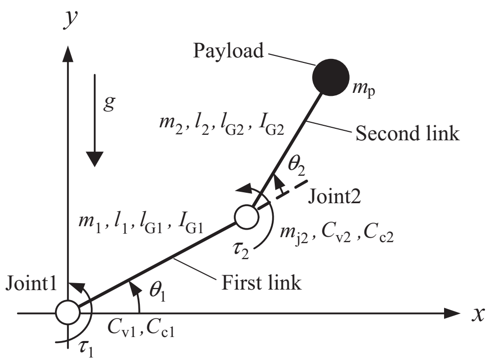

Figure 3: Model of 2-link vertical manipulator

system configuration is described in [2, 3], and the proof of the theorem is described in [2].

Our proposed system shown in Fig. 1 estimates the smoothed value $x_1$ and the differential value $x_2$ from the input signal $y$. The actual implementation is as follows:

$$\begin{cases} \dot{x}_1 = x_2 \\ \dot{x}_2 = -UR^2 \mathrm{sat}\{(S(x_1 - y) + x_2)/\phi\} \end{cases} \tag{2}$$

where $UR^2$, $S$ and $\phi$ are the design parameters, and the sat() indicates the saturation function and is defined by the following equation.

$$\mathrm{sat}(\sigma/\phi) = \begin{cases} \sigma/\phi & |\sigma| < \phi \\ \mathrm{sign}(\sigma) & |\sigma| \geq \phi \end{cases} \tag{3}$$

Figure 2 shows the block diagram of the PID-DAC, and it utilizes the ESDS as a differential estimator. In this figure, $\dot{\theta}_e$ indicates the differential value of the encoder by using ESDS, and $\ddot{\theta}_e$ indicates a second-order differential value by using ESDS twice. A low pass filter (LPF) is applied to the input torque in order to eliminate high frequency elements.

## 3. Apply online-system-identification to the PID-DAC

### 3.1. Modeling of controlled object

Figure 3 shows model of a 2-link vertical manipulator, where $m$ is the mass of the link, $l$ is the length of the link, $l_G$ is the length between the joints and center of gravity of the link, $I_G$ is the moment of inertia about the center of gravity, $C_v$ is the viscous damping coefficient of a joint, $C_c$ is the coulomb friction coefficient of the joint, $\theta$ is the joint

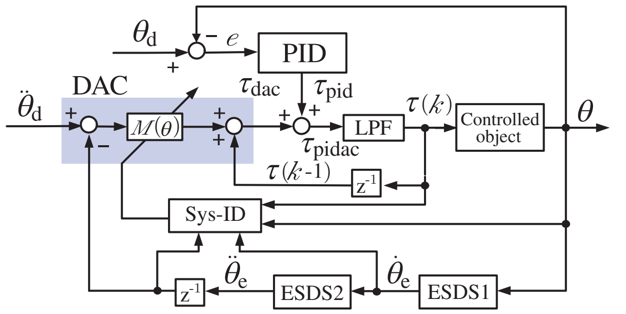

Figure 4: Combined control system of PID and DAC with system identification method

angle, and $\tau$ is the input torque to the joint. Here, suffix 1 and 2 shows first and second links respectively. $m_p$ is the mass of the payload, $m_{j2}$ is the mass of the second joint, and $g$ is gravity force. The following equation is derived using the Lagrange equation:

$$\begin{bmatrix} J_1 + J_2 + J_3\cos\theta_2 & J_2 + \frac{1}{2}J_3\cos\theta_2 \\ J_2 + \frac{1}{2}J_3\cos\theta_2 & J_2 \end{bmatrix} \begin{bmatrix} \ddot{\theta}_1 \\ \ddot{\theta}_2 \end{bmatrix} + \begin{bmatrix} -\frac{1}{2}J_3\dot{\theta}_2(2\dot{\theta}_1 + \dot{\theta}_2)\sin\theta_2 \\ \frac{1}{2}J_3\dot{\theta}_1^2\sin\theta_2 \end{bmatrix} + \begin{bmatrix} J_4\dot{\theta}_1 + J_5\mathrm{sign}(\dot{\theta}_1) \\ J_6\dot{\theta}_2 + J_7\mathrm{sign}(\dot{\theta}_2) \end{bmatrix} + \begin{bmatrix} J_8\cos\theta_1 + J_9\cos(\theta_1 + \theta_2) \\ J_9\cos(\theta_1 + \theta_2) \end{bmatrix} = \begin{bmatrix} \tau_1 \\ \tau_2 \end{bmatrix} \tag{4}$$

where the parameters from $J_1$ to $J_9$ are as follows:

$$\begin{aligned} J_1 &= m_1 l_{G1}^2 + (m_2 + m_{j2} + m_p)\, l_1^2 + I_{G1}, \\ J_2 &= m_2 l_{G2}^2 + m_p l_2^2 + I_{G2}, \\ J_3 &= 2m_2 l_1 l_{G2} + 2m_p l_1 l_2, \\ J_4 &= C_{v1}, \quad J_5 = C_{c1}, \quad J_6 = C_{v2}, \quad J_7 = C_{c2}, \\ J_8 &= \left(m_1 l_{G1} + m_{j2} l_1 + m_2 l_1 + m_p l_1\right) g, \\ J_9 &= \left(m_2 l_{G2} + m_p l_2\right) g. \end{aligned}$$

Equation (4) is rewritten by using the state vectors $\boldsymbol{\theta}$ and $\boldsymbol{\tau}$:

$$\boldsymbol{M}(\boldsymbol{\theta})\ddot{\boldsymbol{\theta}} + \boldsymbol{h}(\boldsymbol{\theta}, \dot{\boldsymbol{\theta}}) = \boldsymbol{\tau}, \tag{5}$$

where $\boldsymbol{\theta} = [\theta_1 \;\; \theta_2]^T$, $\boldsymbol{\tau} = [\tau_1 \;\; \tau_2]^T$ and $\boldsymbol{M}$ is the inertia matrix defined as follows:

$$\boldsymbol{M}(\boldsymbol{\theta}) = \begin{bmatrix} J_1 + J_2 + J_3\cos\theta_2 & J_2 + \frac{1}{2}J_3\cos\theta_2 \\ J_2 + \frac{1}{2}J_3\cos\theta_2 & J_2 \end{bmatrix} \tag{6}$$

### 3.2. Online-system-identification

PID-DAC control system has robustness against modeling errors that are caused by gravity, friction, interaction of joints, and other factors. However, control performance of PID-DAC would deteriorate if there is a modeling error in the inertia matrix. For example, the inertia matrix can be easily changed by changing the payload of the manipulator. This is a big problem. To solve this problem, we apply online system identification algorithm to the PID-DAC control system, and we perform online estimation of the inertia matrix. The physical parameters $J_1, J_2, \cdots, J_9$ are calculated by using the iterative least squares technique. At

Table 1: Specification of manipulator

| First link | | Second link | |
|---|---|---|---|
| $m_1$ | 0.112 kg | $m_2$ | 0.150 kg |
| $m_{j2}$ | 0.410 kg | $m_p$ | 0.100 kg |
| $l_1$ | 0.14 m | $l_2$ | 0.150 m |
| $l_{G1}$ | 0.0625 m | $l_{G2}$ | 0.0750 m |
| $I_{G1}$ | $5.56 \times 10^{-4}$ kg·m$^2$ | $I_{G2}$ | $2.81 \times 10^{-4}$ kg·m$^2$ |
| $C_{v1}$ | $1.22 \times 10^{-4}$ N·m·s | $C_{v2}$ | $1.22 \times 10^{-4}$ N·m·s |
| $C_{c1}$ | $1.20 \times 10^{-2}$ N·m | $C_{c2}$ | $1.20 \times 10^{-2}$ N·m |
| resolution | $2\pi/4000$ | resolution | $2\pi/4000$ |

Table 2: Parameters of the control system

| | | | |
|---|---|---|---|
| $UR_1^2$ | 1500 | $UR_2^2$ | 1500 |
| $S_1$ | 160 | $S_2$ | 150 |
| $\phi_1$ | 2 | $\phi_2$ | 20 |
| $\boldsymbol{K}_p$ | diag(1.5, 1.5) | $\boldsymbol{K}_i$ | diag(0.05, 0.05) |
| $\boldsymbol{K}_d$ | diag(1.5, 1.5) | | |
| $\boldsymbol{\sigma}_0$ | $\boldsymbol{0}$ | $\boldsymbol{P}_0$ | diag(100, ..., 100) |

the beginning, Eq. (4) is rewritten as $\boldsymbol{\Lambda\sigma} = \boldsymbol{\tau}$, where,

$$\boldsymbol{\Lambda} = \begin{bmatrix} \lambda_{11} & \lambda_{12} & \lambda_{13} & \cdots & \lambda_{19} \\ \lambda_{21} & \lambda_{22} & \lambda_{23} & \cdots & \lambda_{29} \end{bmatrix}, \quad (7)$$

$$\boldsymbol{\sigma} = \begin{bmatrix} J_1 & J_2 & \cdots & J_9 \end{bmatrix}^T, \quad (8)$$

and each component of the matrix $\boldsymbol{\Lambda}$ are as follows:

$$\lambda_{16} = \lambda_{17} = \lambda_{21} = \lambda_{24} = \lambda_{25} = \lambda_{28} = 0,$$
$$\lambda_{11} = \ddot{\theta}_1, \quad \lambda_{12} = \lambda_{22} = \ddot{\theta}_1 + \ddot{\theta}_2,$$
$$\lambda_{14} = \dot{\theta}_1, \quad \lambda_{15} = \mathrm{sign}(\dot{\theta}_1),$$
$$\lambda_{26} = \dot{\theta}_2, \quad \lambda_{27} = \mathrm{sign}(\dot{\theta}_2),$$
$$\lambda_{18} = \cos(\theta_1), \quad \lambda_{19} = \lambda_{29} = \cos(\theta_1 + \theta_2),$$
$$\lambda_{13} = \cos\theta_2 \cdot \ddot{\theta}_1 + \frac{1}{2}\cos\theta_2 \cdot \ddot{\theta}_2 - \frac{1}{2}\dot{\theta}_2(2\dot{\theta}_1 + \dot{\theta}_2)\sin\theta_2,$$
$$\lambda_{23} = \frac{1}{2}\cos\theta_2 \cdot \ddot{\theta}_1 + \frac{1}{2}\dot{\theta}_1^2 \sin\theta_2. \quad (9)$$

$\boldsymbol{\Lambda}$, $\boldsymbol{\tau}$, and $\boldsymbol{\sigma}$ are represented as $\boldsymbol{\Lambda}_i$, $\boldsymbol{\tau}_i$, and $\boldsymbol{\sigma}_i$ respectively when time $t = t_i$. By using these parameters, the iterative least squares algorithm for estimating the physical parameters is derived:

$$\boldsymbol{\sigma}_N = \boldsymbol{\sigma}_{N-1} - \boldsymbol{P}_N \boldsymbol{\Lambda}_N^T(\boldsymbol{\Lambda}_N \boldsymbol{\sigma}_{N-1} - \boldsymbol{\tau}_N), \quad (10)$$

$$\boldsymbol{P}_N = \boldsymbol{P}_{N-1} - \boldsymbol{P}_{N-1}\boldsymbol{\Lambda}_N^T(\boldsymbol{I} + \boldsymbol{\Lambda}_N \boldsymbol{P}_{N-1}\boldsymbol{\Lambda}_N^T)^{-1}\boldsymbol{\Lambda}_N \boldsymbol{P}_{N-1}. \quad (11)$$

At the beginning, the initial values $\boldsymbol{\sigma}_0$ and $\boldsymbol{P}_0$ are given and the input and output data ($\boldsymbol{\tau}_1$ and $\boldsymbol{\Lambda}_1$) are obtained. Then a new physical parameter $\boldsymbol{\sigma}_1$ is calculated by using Eq. (10), and a parameter $\boldsymbol{P}_1$ is calculated by using Eq. (11). By repeating the procedure, we can update physical parameters. Figure 4 shows the PID-DAC after applying system identification method.

## 4. Simulation results

We applied the proposed method to the 2-link vertical manipulator as shown in Fig. 3. Table 1 and 2 shows manipulator specifications and parameters of the control system respectively. The desired angle for each joint is $\theta_d(t) = 0.7\sin(2\pi t/5)$. A low pass filter (LPF) is applied to the input torque in order to eliminate high frequency elements since the differential estimator works as a high pass filter. For the LPF, first-order Butterworth filter with a cut-off frequency of 4Hz is used. In order to confirm the robustness of the proposed algorithm, payload is changed from 100g to 250g at time 7.5s.

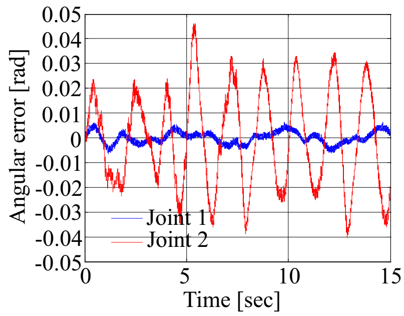

Figure 5: Angular error: PID control, horizontal plane

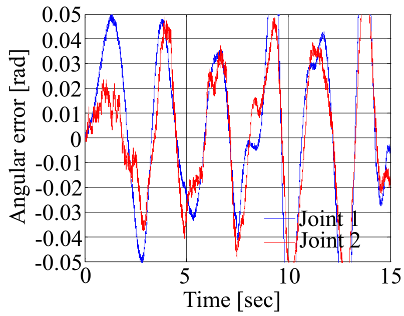

Figure 6: Angular error: PID control, vertical plane

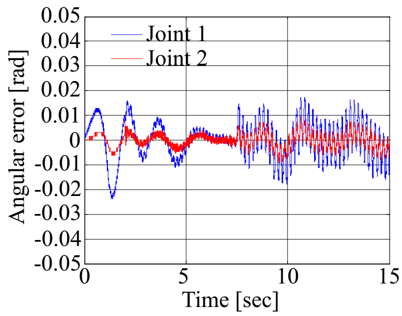

Figure 7: Angular error: PID-DAC control, vertical plane

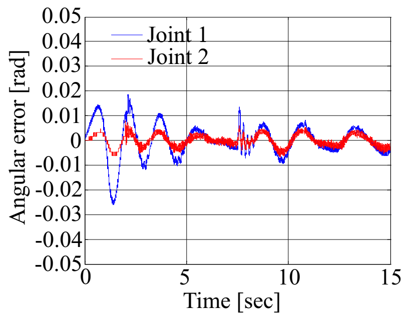

Figure 8: Angular error: PID-DAC with system identification, vertical plane

Figures 5 and 6 show angular errors that are obtained by using the conventional PID controller. Attitude of the

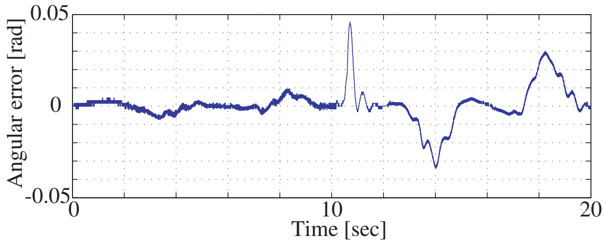

Figure 9: Angular error: PID control, vertical plane, joint-2

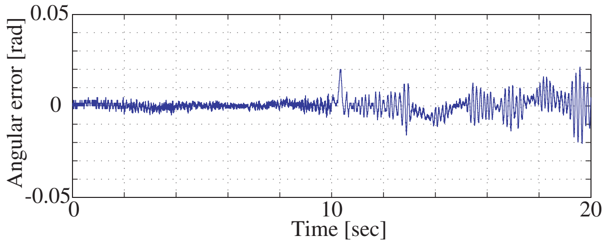

Figure 10: Angular error: PID-DAC, vertical plane, joint-2

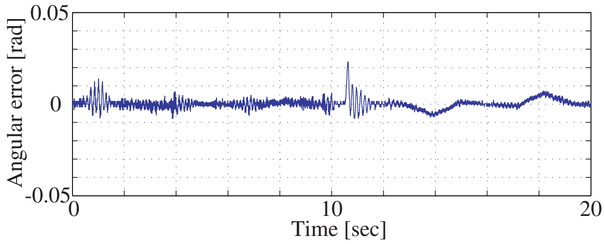

Figure 11: Angular error: PID-DAC with system identification, vertical plane, joint-2

manipulator is horizontal in the case of Fig. 5, and vertical in the case of Fig. 6. It can be concluded that the control performance shown in Fig. 6 is inferior to Fig. 5. The difference of the results obtained in Figs. 5 and 6 is an influence of gravity term, namely an influence of nonlinear term. These results show that the PID control system cannot work properly under the influence of nonlinear term.

Figure 7 shows angular errors obtained by applying the PID-DAC controller to the vertical manipulator. It shows that the PID-DAC controller has a good robustness against nonlinear terms. However, high frequency vibrations occur at time $t$=7.5s, which can destabilize the control system.

Figure 8 shows angular errors obtained by applying the PID-DAC controller with system identification algorithm to the vertical manipulator. It shows a better control performance than those obtained in Fig. 7, even with payload changes. On comparing results for time taken to calculate the physical parameters for the online system identification algorithm with the offline system, the online system took 0.076ms, whereas, for the offline system the time taken is 1.2ms. It is because the offline system requires a calculation of 500 input and output data to obtain physical parameters. These results show that the calculation time is significantly reduced by applying the online system identification algorithm. In general, the sampling time of the mechanical system is a few milliseconds and for our proposed method the calculation time is short enough to be implemented to a mechanical system.

## 5. Experimental results

Experiments were performed on the simulation conditions. For the experiment, a payload of 150g was added at about 10s. Figures 9, 10 and 11 shows angular errors of joint 2, when the attitudes of the manipulator are vertical. The controller for Figs. 9–11 are PID, PID-DAC and PID-DAC with system identification respectively. These results shows that the control performance of the proposed method are superior to the conventional PID and PID-DAC algorithm.

The sampling period of the simulations and experiments is 2ms. We can implement the proposed algorithm to the actual equipment by using a common digital signal processor. The proposed method can be applied to wide area of mechanical systems.

## 6. Conclusions

This paper presents performance improvements of PID-DAC by applying the online system identification. The validity of the proposed method was confirmed by performing simulations and experiments using a 2-link manipulator. The results show the validity of the proposed method from the viewpoints of control performances. Furthermore, the calculation time is short enough to realize real time control.

## References

[1] S.Y. Wang, K. Takahashi, Y. Hashimoto, K. Hori, T. Tsuchiya, and M. Nakatsuyama, "The Estimation Method Velocity and Acceleration Using Fuzzy Reasoning and its Application to Robot Manipulator Trajectory Control," *Fuzzy Theory and System*, vol.8, no.2, pp.571–583, 1997.

[2] T. Emaru and T. Tsuchiya, "Research on Estimating Smoothed Value and Differential Value By Using Sliding Mode System," *IEEE Trans. on Robotics and Automation*, vol.19, no.3, pp.391–402, 2003.

[3] T. Emaru and T. Tsuchiya, "Research on Parameter Determination for Smoothed and Differential Value Estimator," *IEICE Transactions*, vol.E86-A, no.7, pp.1732–1741, 2003.

[4] A. Levant, "Robust exact differentiation via sliding mode technique," *Automatica*, vol.34, no.3, pp.379–384, 1998.

[5] A. Levant, "Higher-order sliding modes, differentiation and output-feedback control," *International Journal of Control*, vol.76, no.9/10, pp.924–941, 2003.

[6] K. Imagawa, T. Emaru, Y. Hoshino, and Y. Kobayashi, "Estimation of velocity and acceleration by nonlinear filter based on sliding mode and application to control system," *in Proc. Asia Int. Symposium on Mechatronics*, pp.212–217, 2008.

[7] T. Emaru, K. Imagawa, Y. Hoshino and Y. Kobayashi, "Development of Control System by Nonlinear Compensation using Digital Acceleration Control," *in Proc. ASME Dynamic Systems and Control Conference*, DSCC2010-4125, 2010.